Spring 3-11-2019

Studies of Boundary Layer Transition from Laminar to Turbulent

Elizabeth Spaulding
University of Nebraska - Lincoln

Studies of Boundary Layer Transition from Laminar to Turbulent

An Undergraduate Honors Thesis
Submitted in Partial Fulfillment of
University Honors Program Requirements
University of Nebraska-Lincoln

by
Elizabeth Spaulding, B.S.
Mathematics
College of Arts and Sciences

March 11, 2019

Faculty Mentors:
Adam Larios, PhD, Mathematics
Jae Sung Park, PhD, Mechanical Engineering

Abstract

In engineering applications, there is a strong desire to reduce energy losses due to turbulent energy production. However, the theoretical understanding of turbulent and transition flow is still lacking due to the absence of an exact mathematical solution for turbulent flow. In the current project, transition and turbulent behavior in wall-bounded flow is studied, with an emphasis on concepts from boundary layer theory. Organized structures, such as streaks, waves, and vortices, which occur in such flows, are analyzed. Especially for near-wall structures, control strategies for suppressing such structures are discussed. Using mathematical equations which govern fluid flow, models for different behaviors are derived, studied, and simulated computationally. Peer-reviewed literature covering these topics is given a careful review and is used as a point of comparison for the results of the current study. Fundamentals of the structure of the boundary layer are given, noting flow separation's role in producing wake turbulence. Simulations of turbulent channel flow were run at varying conditions with the goal of studying how changing properties of flow at the wall affects transition and turbulence. Results of the current study include analysis of mean velocity and wall shear stress profiles, analysis of flow structures, and observations of the dependence of the Reynolds number on the time for transition from laminar to turbulent flow.

Key Words: turbulence control, transition flow, boundary layer, coherent structures, vortices, fluid dynamics

1 Introduction

In fluid dynamics, turbulent flow is still not well understood mathematically. While turbulence can be studied experimentally in wind tunnels and simulated numerically, much of the behavior of turbulent flow is unpredictable. Study of turbulent behavior, specifically the turbulent boundary layer, may lead to insight in turbulence control and how to reduce skin friction drag in various engineering applications. For example, in aircraft and ships, skin friction drag makes up a large fraction of the total drag. Reducing skin friction drag would result in reductions in operational cost for airlines and shipping industries, as well as enabling increased speed, range, and endurance. Other major applications of turbulence control are reduction of energy losses in pipelines, enhanced mixing in combustion engines, enhanced heat transfer in heat exchanges, and improved efficiency of heating and cooling systems.

Much of the literature in turbulent boundary layer theory proposes the presence of organized structures - such as hairpin vortices, turbulent puffs, and traveling waves - which account for most of the energy in turbulent fluctuations. Current studies aim to reduce turbulent drag in many applications using control strategies focusing on manipulation of near-wall turbulent structures. For example, Choi et al.[1] used suction and blowing at the wall using velocity information from inside the flow. This control scheme was successful in reducing turbulent drag by suppressing the turbulent structures near the wall. However, the scheme is impractical as velocity information inside the flow is not readily available. Many control strategies use blowing and suction at the wall - an active wall motion such as blowing and suction is one of the most practical ways to reduce skin friction drag thus far.

The transition from laminar flow to turbulent flow is another topic under close scrutiny by fluid dynamicists. According to Eckhardt et al.[3], conditions which can trigger the transition to turbulence are a sufficiently fast flow (leading to a higher Reynolds number), or sufficiently strong perturbations to the flow. Eckhardt et al. notes that coherent structures and flow patterns such as hairpin vortices first appear during the transition to turbulence, and grow as the flow becomes more turbulent. The presence of structures such as these can give a good indication of when transition actually begins - though, as noted in the study, a precise Reynolds number dictating when transition begins is not easy to identify. One engineering application for studying the transition to turbulence is the desire to delay transition in a flow to reduce skin friction drag.

The goal of the current project is to investigate how the physics and conditions affect turbulent and transitional behavior, as well as explore control schemes in wall-bounded turbulent flow. In order to establish a thorough foundation in the science of fluid dynamics as a whole, laminar and transition flow will be studied, as well as mathematical and computational models for flows at different Reynolds numbers. Ultimately, we will research how changing properties of the flow at the wall will affect turbulent flow using equations governing fluid flow.

2 Literature Review

The best mathematical model for fluid flow is given by the Navier-Stokes equations, three nonlinear partial differential equations which still have no precise mathematical solution today. These are the governing equations of fluid dynamics. Because there is no exact mathematical solution, fluid dynamicists use direct numerical simulations (DNS) to approximate the solutions to these equations in order to model fluid flow computationally. The two-dimensional Navier-Stokes equations are given by:

$$\begin{aligned} \text{X: } & \frac{\partial u}{\partial t} + u\frac{\partial u}{\partial x} + v\frac{\partial u}{\partial y} = -\frac{1}{\rho}\frac{\partial p}{\partial x} + \nu(\frac{\partial^2 u}{\partial x^2} + \frac{\partial^2 u}{\partial y^2}) \\ \text{Y: } & \frac{\partial v}{\partial t} + u\frac{\partial v}{\partial x} + v\frac{\partial v}{\partial y} = -\frac{1}{\rho}\frac{\partial p}{\partial y} + \nu(\frac{\partial^2 u}{\partial x^2} + \frac{\partial^2 u}{\partial y^2}) \\ \text{Continuity: } & \frac{\partial u}{\partial x} + \frac{\partial v}{\partial y} = 0 \end{aligned} \tag{1}$$

The boundary layer is a very thin layer that forms when fluid adjacent to the surface of an object moving through fluid (or an object with fluid moving past it) sticks to the surface. Boundary layer theory dictates that frictional effects are only observed within the boundary layer. As the boundary layer travels down the object, it separates from the object in a phenomenon called flow separation, causing vortices to form in the gap between the surface and the separated boundary layer. This is what causes wake turbulence. Thus, simulations of the turbulent boundary layer allow study of wake turbulence.

Earlier experimental and computational studies provided limited evidence for turbulent structures. An important survey of coherent structures in the turbulent boundary layer was given by Robinson[9]. Robinson identified some key issues of controversy in boundary layer research: the near-wall bursting process of turbulence production, and the existence of hairpin vortices. Hairpin vortices were described as rare in low Reynolds-number simulations. Experimental methods using dye, particles, bubbles, and smoke to observe turbulent structures such as hairpin vortices were limited to low Reynolds numbers and were generally not quantitative, therefore producing ambiguous results. However, quantitative studies of turbulent structures could be accomplished through the use of DNS, which were also limited to low Reynolds-number flows with simple geometries due to being computationally expensive.

More recently, Wu & Moin provided a good model for a turbulent zero-pressure-gradient incompressible boundary layer over a smooth flat plate (ZPGFPBL)[12]. This study aimed to create an accurate dataset for the turbulent ZPGFPBL by computing a laminar Blasius boundary layer from $Re_\theta = 80$ to a low Reynolds-number ($Re_\theta < 1000$) turbulent ZPGFPBL. A spatially developing approach was taken in this experiment - that is, unlike many previous studies, they neither invoked non-physical streamwise periodicity nor added terms to the Navier-Stokes equations. Patches of isotropic turbulence were periodically introduced to the flow at the inlet. This DNS followed closely statistically with previous DNS of turbulent boundary layers. The boundary layer remained consistent with the Blasius model from

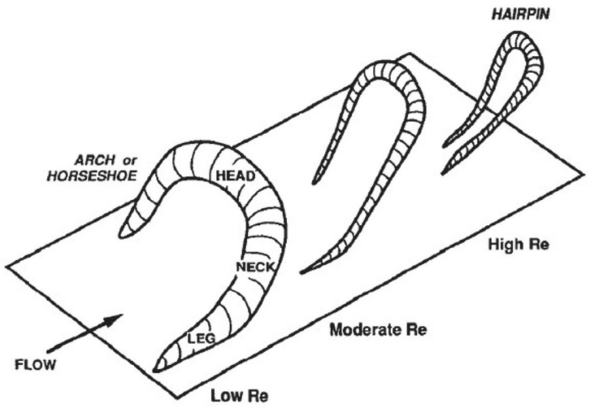

Figure 1: Hairpin vortices from Robinson[9] after Head & Bandyopadhyay[5].

$80 < Re_\theta < 180$, with transition flow completing at around $Re_\theta = 750$. The results of this experiment are notable due to the discovery of the dominance of hairpin vortices in the instantaneous flow fields, suggesting that they development of turbulent flow and hairpin vortices are correlated.

Interestingly, He & Seddighi[4] investigated low-Reynolds number turbulent flow through a channel using DNS and found that, subject to a large increase in flow rate, the flow underwent a transition similar to boundary layer bypass transition induced by free-stream turbulence (FST). Bypass transition is a transition to turbulence which occurs when transitional phenomena such as Tollmien-Schlichting waves are bypassed, causing the transition to occur much more rapidly and at much lower Reynolds numbers. Before this transition, elongated streaky structures were observed, becoming more elongated as the flow developed. As turbulent regions grew and spread, more typical turbulent structures were observed as the energy grew and the streaks were broken up.

Our project focuses on incompressible, wall-bounded turbulent flow, with an emphasis on observing phenomena of transition flow. This sort of model, similar to plane Poiseuille flow, emulates flow through a channel, or perhaps a pipe. Much of the turbulent energy production takes place in the region near the wall, where the presence of organized flow structures has been found in various studies. Prandtl, known for introducing the boundary layer concept, postulated that the mean velocity profile near the wall is determined by viscous scales at high Reynolds numbers, independent of the flow away from the wall.

The momentum transfer by the fluctuating velocity field causes Reynolds stress[8], accounting for turbulence in fluid flow. High skin-friction drag in turbulent boundary layers and channel flows such as plane Poiseuille flows is caused by near-wall quasi-streamwise vortices (QSVs)[1], which are a direct result of this fluctuating velocity field. These structures are known as streaks, and are unstable because of the spanwise gradient of the streamwise velocity - consisting of wall-normal and spanwise velocities, independent of the streamwise direction, they interact with the mean shear dU/dy and create a dependence in the streamwise velocity near the wall. Streaks create even more vertices in the following

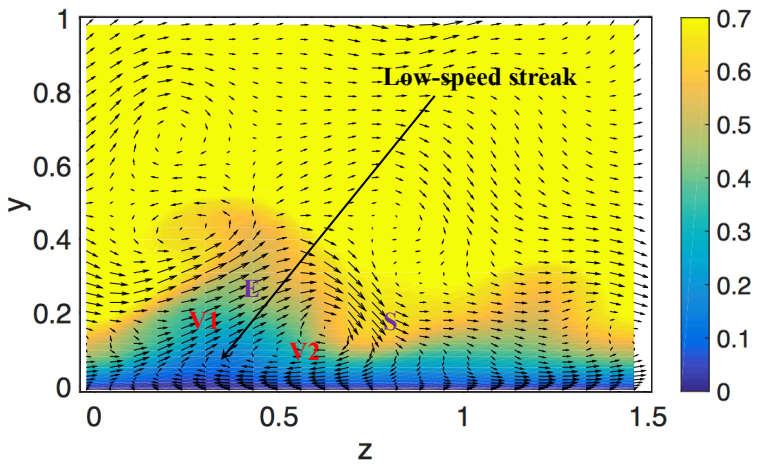

Figure 2: Velocity distributions in the y-z plane lower half of the channel in a plane Poiseuille flow. The streamwise component is represented by the colored contours and the wall-normal and spanwise components are shown by arrows. Two streamwise vortices, $V1$ and $V2$, are shown, and the two events, E and S that result from them are shown as well. Note also the low-speed streak forming at the bottom of the graph. This is also a result of the streamwise vortices shown.

self-sustaining[7][10][11] process: the streaks migrate slowly from the wall, exhibit rapid oscillations, and then break down. This entire process is unaffected by the outer part of the boundary layer at low Reynolds numbers. We call the part when the streaks migrate from the wall ejection events - these are accompanied by sweep events. In sweep events, high-momentum fluids are induced towards the wall, creating areas of high wall shear stress. According to Pope, the majority of turbulent energy production occurs during this area during the sweep and ejection events[8].

In figure 2, we see the velocity distributions in the y-z plane in the lower half of the channel. The contours show the streamwise component (u), while the wall-normal (v) and spanwise (w) components are shown by arrows, scaled by the laminar centerline velocity. The horizontal axis represents the wall and the vertical axis represents the friction Reynolds number. Observe $V1$ and $V2$, two streamwise vortices that have formed. E denotes an ejection event, while S denotes a sweep event. Notice that $V1$ brings high-momentum fluid from the flow toward the wall, while lifting low-momentum fluid away from the wall. The former is a sweep event and the latter, an ejection event. This causes the formation of a low-speed streak. These vortical structures, and their effects on the mean flow, create regions of local wall shear stress. In particular, the sweep events create high skin friction zones while the ejection events create low skin friction zones. A natural progression from this data is the desire to manipulate the interactions between these vortices and the wall in order to suppress these sweep and ejection events. In fact, many studies have attempted use various control strategies (such as blowing and suction at the wall) to reduce such interactions with some success.

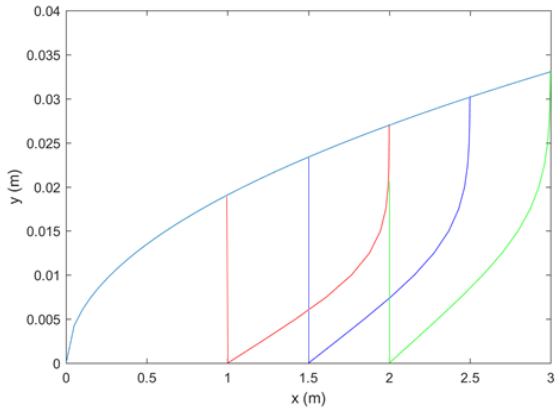

Figure 3: A Blasius boundary layer for 1.0m/s air flow over a 3m-long surface, with inner velocity profiles. The upper curve is the boundary layer thickness, which we denote by δ_{99}. The colored profiles underneath that curve represent the velocity profiles - the straight vertical lines indicate the start point of the velocity vectors and the curves indicate the end points. Note that the widening profiles show that the lengths of the velocity vectors increases as y increases.

3 Fundamentals of the Boundary Layer Structure

As previously stated, the boundary layer, first proposed by Prandtl, is a very thin layer that forms when fluid adjacent to the surface sticks to the surface. Viscous effects are only observed within the boundary layer. The Blasius boundary layer is a two-dimensional, steady-state, incompressible boundary layer on a plate parallel to laminar flow in one direction. A Blasius boundary layer for 1.0m/s flow over a flat surface can be seen plotted in figure 3. Notice the velocity profiles: as y increases, the inner velocities increase until they hit the boundary layer thickness, denoted by δ_{99}. This δ_{99} is named such because we define the boundary layer to stop when the inner velocity reaches 99% of the outer velocity. As x increases, the velocities decrease. In fact, flow separation is said to occur when the gradient of the velocities approaches 0.

We quickly derive the Blasius solution using the two-dimensional Navier-Stokes equations (as seen in equation (1)). For the Blasius solution, we assume the following, for u the inner velocity component in the streamwise direction, v in the spanwise direction, and U the outer velocity component in the streamwise direction:

$$\begin{aligned} u &\gg v \\ \frac{\partial}{\partial y} &\gg \frac{\partial}{\partial x} \\ Re &\gg 1 \\ U &= constant \end{aligned} \tag{2}$$

By our scaling assumptions, and the assumption that the Blasius boundary layer is steady-state, we get

the following equations by eliminating terms from the Navier-Stokes equations (equation (1)) which go to zero:

$$\begin{aligned} \text{Momentum} : u\frac{\partial u}{\partial x} + v\frac{\partial u}{\partial y} &= -\frac{1}{\rho}\frac{\partial p}{\partial x} + \nu\frac{\partial^2 u}{\partial y^2} \\ \text{Continuity} : \frac{\partial u}{\partial x} + \frac{\partial v}{\partial y} &= 0 \end{aligned} \tag{3}$$

Now, by the Bernoulli equation, we may find that the pressure derivative in the x-direction is zero. So, now, we have:

$$\begin{aligned} \text{Momentum} : u\frac{\partial u}{\partial x} + v\frac{\partial u}{\partial y} &= \nu\frac{\partial^2 u}{\partial y^2} \\ \text{Continuity} : \frac{\partial u}{\partial x} + \frac{\partial v}{\partial y} &= 0 \end{aligned} \tag{4}$$

And, as per the problem statement for the Blasius boundary layer, we have the following Boundary conditions:

$$\begin{aligned} u = 0 \text{ at } y = 0 \\ v = 0 \text{ at } y = 0 \\ u \to U \text{ as } y \to \infty \end{aligned} \tag{5}$$

We now introduce the similarity variable η, which couples x and y together, and the stream function, ψ.

$$\begin{aligned} \eta = \frac{y}{\delta} = \frac{y}{(\nu x/U)^{1/2}} \\ \psi = U\delta f(\eta) \to u = \frac{\partial \psi}{\partial y}, v = -\frac{\partial \psi}{\partial x} \end{aligned} \tag{6}$$

Finally, we plug the similarity variable and stream function into the boundary layer equations. Using the chain rule, we derive the Blasius equation:

$$\begin{aligned} f''' + \frac{1}{2}ff'' = 0 \\ f = f' = 0 \text{ at } \eta = 0 \\ f' = 1 \text{ as } \eta \to \infty \end{aligned} \tag{7}$$

This equation was used to plot the δ_{99} curve of a 1.0m/s Blasius boundary layer over a flat surface as you saw in figure 3 using the Runge-Kutta method and secant method in Matlab. Another similar solution, derived from the Blasius solution, is the Falkner-Skan solution, which simply allows us to model the Blasius boundary layer over a non-flat surface. As the change to the equations are minimal, we won't include that here.

Now, as the boundary layer travels down the object, the gradient of the inner velocity relative to the object decreases until it goes to nearly 0. At this point, flow separation occurs. That is, the boundary

layer separates from the object, creating a gap between the surface of the object and the boundary layer. Within this gap, vortices form. This phenomenon is said to cause wake turbulence, which, in turn, causes large amounts of drag. It is desirable, then, to attempt to suppress this flow separation.

4 Simulation Details

The simulation run for this project is that for three-dimensional flow through a channel, modeled after plane Poiseuille flow. That is, the flow geometry is a rectangular domain bounded by a top and bottom wall. The x coordinate is aligned with the streamwise direction, the y coordinate is aligned with the wall-normal direction, and the z coordinate is aligned with the spanwise direction. No-slip boundary conditions are applied at the walls and periodic boundary conditions are applied in the x and z directions. The periods are the same as the box dimensions in the corresponding directions - L_x and L_y respectively. Half-channel height, i.e. $L = L_y/2$ is chosen as the length scale for non-dimensionalization. The velocity scale is the Newtonian laminar centerline velocity $U = \frac{3}{2}U_{bulk}$, where U_{bulk} is the bulk velocity in the Newtonian laminar flow. We chose a constant $U_{bulk} = \frac{2}{3}$. Time t is scaled with L/U, and pressure p with ρU^2, where ρ is the fluid density. The non-dimensional governing equations, then, are given as:

$$\begin{aligned} \frac{\partial u}{\partial t} + u \cdot \nabla u &= -\nabla p + \frac{1}{Re}\nabla^2 u \\ \nabla \cdot u &= 0 \end{aligned} \tag{8}$$

Here, $Re = LU/\nu$, where ν is the kinematic viscosity of the fluid. The friction Reynolds number, Re_τ, is defined as $Re_\tau = Lu_\tau/\nu$, where $u_\tau = \sqrt{\tau_w/\rho}$ is the friction velocity; τ_w is the time- and area-averaged wall shear stress. We used Gibson's channel flow code to solve the governing equations.

We measure the strength of the streamwise vortices by adapting the Q-criterion[2][6][13] of vortex identification to the two-dimensional y-z plane[14]: $Q_{2D} \equiv (1/2)(\|\Omega_{2D}\|^2 - \|\Gamma_{2D}\|^2)$, where $\Gamma_{2D} \equiv (1/2)(\nabla v_{2D} + \nabla v_{2D}^T)$ and $\Omega_{2D} \equiv (1/2)(\nabla v_{2D} + \nabla v_{2D}^T)$ are the two-dimensional equivalents of the rate-of-strain and vorticity tensors, and $\nabla v_{2D} \equiv (\frac{\partial v_y}{\partial y}, \frac{\partial v_z}{\partial y}; \frac{\partial v_y}{\partial z}, \frac{\partial v_z}{\partial z})$.

5 Laminar Flow

Wall shear stress, or, τ_w, is a valuable metric for determining flow behavior. A higher wall shear stress indicates turbulent flow. For plane Poiseuille flow, we have that $\tau_w = 2$ when flow is laminar. This fact is reflected in our simulations, as can be observed in figure 6, where the wall shear stress remains at about 2 until transition occurs. We can also theoretically derive this fact using the continuity and momentum equations:

Here, we have the continuity equation. We can cancel out the terms in the v- and w-directions to get:

$$\begin{aligned} \frac{\partial u}{\partial x} + \frac{\partial v}{\partial y} + \frac{\partial w}{\partial z} &= 0 \\ \Rightarrow \frac{\partial u}{\partial x} &= 0 \end{aligned} \tag{9}$$

Here, we have the momentum equation in the x-direction. We can cross out each term that is not $-\frac{1}{\rho}\frac{\partial p}{\partial x}$ to find that the partial derivative of pressure with respect to x is constant:

$$\begin{aligned} \frac{\partial u}{\partial t} + u\frac{\partial u}{\partial x} + v\frac{\partial u}{\partial y} + w\frac{\partial u}{\partial z} &= -\frac{1}{\rho}\frac{\partial p}{\partial x} + \nu(\frac{\partial^2 u}{\partial x^2} + \frac{\partial^2 u}{\partial y^2} + \frac{\partial^2 u}{\partial z^2}) \\ \Rightarrow \frac{\partial p}{\partial x} &= \mu\frac{\partial^2 u}{\partial y^2} = constant \end{aligned} \tag{10}$$

So then, we need to solve the differential equation $\mu\frac{\partial^2 u}{\partial y^2} = 0$. These are our boundary conditions:

$$\begin{aligned} &1 : y = \pm L, u = 0 \\ &2 : \frac{\partial u}{\partial y}|_{y=0} = 0 \end{aligned} \tag{11}$$

We use the second boundary condition (for symmetry) to show that c_1 goes to zero:

$$\begin{aligned} \frac{\partial u}{\partial y} &= \frac{1}{\mu}\frac{\partial p}{\partial x}y + c_1 \\ &= \frac{1}{\mu}\frac{\partial p}{\partial x}y \end{aligned} \tag{12}$$

Now, we use our first boundary condition:

$$\begin{aligned} u &= \frac{1}{2\mu}\frac{\partial p}{\partial x}y^2 + c_2 \\ c_2 &= -\frac{L^2}{2\mu}\frac{\partial p}{\partial x} \\ \therefore u(y) &= -\frac{L^2}{2\mu}\frac{\partial p}{\partial x}(1 - \frac{y^2}{L^2}) \end{aligned} \tag{13}$$

We want to non-dimensionalize our solution:

$$\begin{aligned} u(y) &= -\frac{L^2}{2\mu}\frac{\partial p}{\partial x}(1 - \frac{y^2}{L^2}) \\ U_c &= -\frac{L^2}{2\mu}\frac{\partial p}{\partial x} \\ \Rightarrow \frac{u(y)}{U_c} &= u^* = 1 - y^{*2} \end{aligned} \tag{14}$$

Now, the wall shear stress is defined as

$$\tau_w = \mu\frac{du}{dy}|_{wall} \tag{15}$$

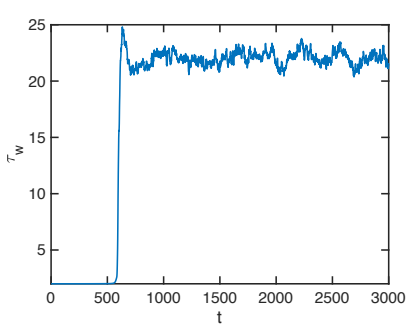

(a) Wall shear stress profile

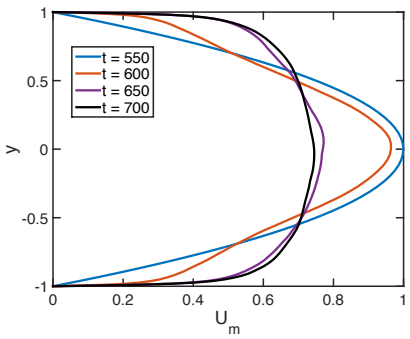

(b) Mean velocity profile as a function of time

Figure 4: Mean profiles

Thus, for laminar flow, we have

$$\tau_w^* = \frac{du^*}{dy^*}|_{wall} = 2 \tag{16}$$

6 Transition to Turbulence

6.1 Mean profiles

Data for mean velocity and wall shear stress profiles was collected. Figure 4a shows the wall shear stress plotted against time. Notice that the flow remains laminar (at around $\tau_w = 2$) until around time $t = 550$, when transition begins to occur. At this point, the wall shear stress jumps dramatically and begins fluctuating, as is consistent with previous literature's indication of transition occurring. Based on analysis of the dominance of coherent structures in the domain, turbulence follows after that at around $t = 600$. As we saw in the previous section, the mean velocity, $u = 1 - y^2$. This is reflected in figure 4b. As time increases and transition begins to occur, the "sideways" parabola shape of the mean velocity becomes more blunt. Notice in figure 5 the strength of the vortices at various time points. At time $t = 550$, we see relatively weak vortices, an indicator of transition beginning. As time increases and transition occurs, the vortices become much stronger and populate much more of the domain. Interestingly, at time $t = 600$, only about half of the domain is heavily populated by vortices. By the time we get to time $t = 700$, it is clear that the flow is truly turbulent due to the dominance of structures in the domain.

6.2 Flow structures

Flow structures occur throughout all stages of transitional flow. As can be seen in graphs of the contours of the wall shear stress in figure 6, as the flow turns from laminar to turbulent, various flow structures form. In figure 6a, we see Tollmien-Schlichting waves form. This gives us a good indication that transition is beginning to occur, as Tollmien-Schlichting waves are common occurrences in transition flow. We

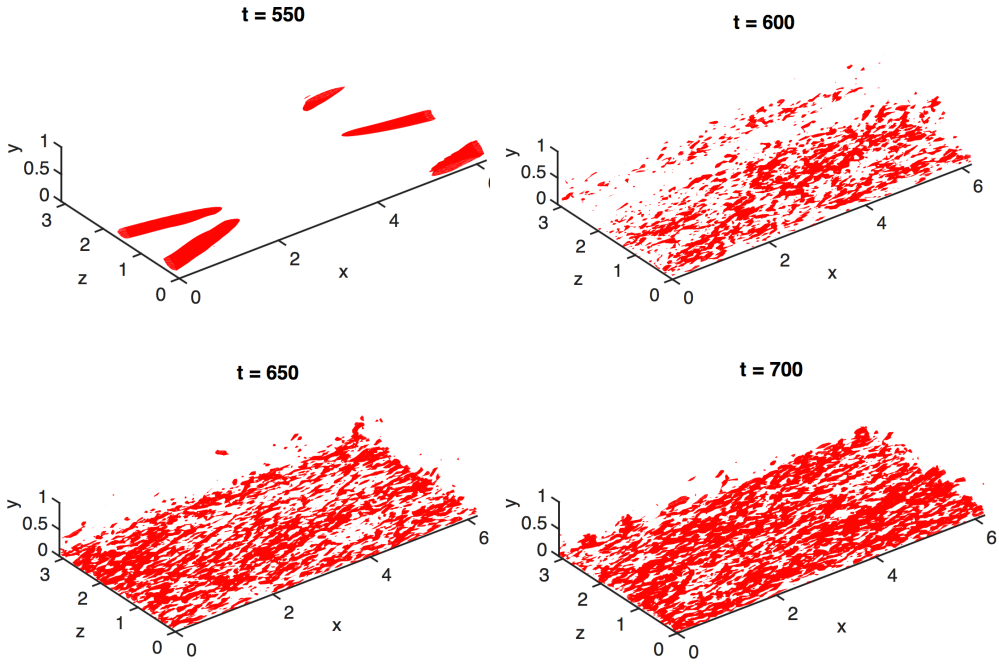

Figure 5: Strength of streamwise vortices

observe greater and greater disturbances and time increases - in figure 6c, about half of the domain is turbulent while the other half remains somewhere in between laminar and turbulent. This is consistent with our expectations of transition flow: not quite turbulent, and not quite laminar. Finally, we observe true turbulent flow when $t > 600$ in figure 6d. Here, the wall shear stress fluctuates chaotically and we see the domain heavily populated by flow structures such as vortices.

6.3 Dependence of Reynolds Number on Transition

Several simulations were ran at different Reynolds numbers to determine transition times. Five such simulations were ran at increasing Reynolds numbers $Re_1 = 15,000$, $Re_2 = 17,500$, $Re_3 = 20,000$, $Re_4 = 22,500$, and $Re_5 = 25,000$. We define the approximate time point at which transition occurs to be the sudden spike in wall shear stress, as can be observed in figure 7. Interestingly, as the Reynolds number increased, transition from laminar flow to turbulence was delayed, as can be seen in figure 8. As the Reynolds number increases each step by 2,500, time to transition seems to increase quite quickly. Surprisingly, the graph almost looks parabolic. This leads us to believe that transition time is dependent upon the Reynolds number in perhaps unexpected ways. Because of these unexpected results, we hesitate to draw conclusions. This dependency of transition time on the Reynolds number will be a topic of future work, along with studying other methods and conditions which could enable us to delay transition time.

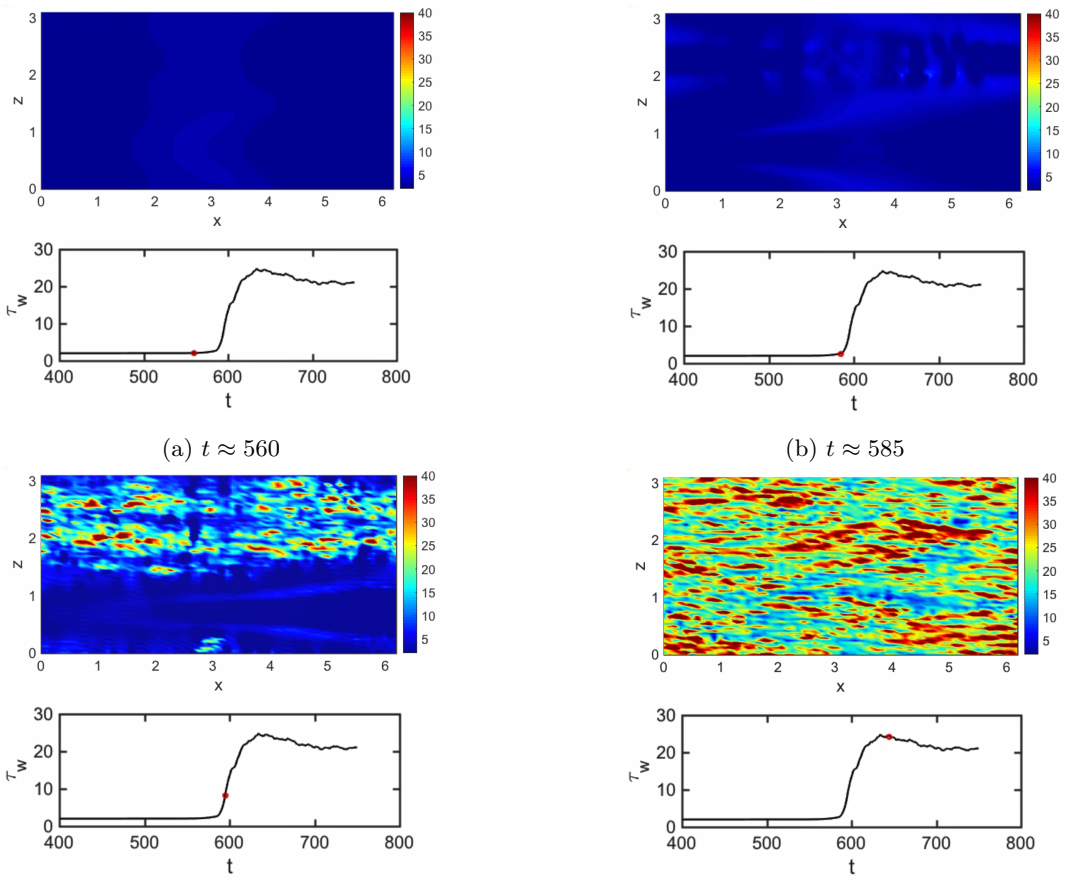

(a) $t \approx 560$

(b) $t \approx 585$

(c) $t \approx 599$

(d) $t > 600$

Figure 6: Contours of the wall shear stress τ_w at different times throughout transition, paired with graphs showing τ_w's current position in time and in a broader context. Flow structures can be seen throughout various times by these contours.

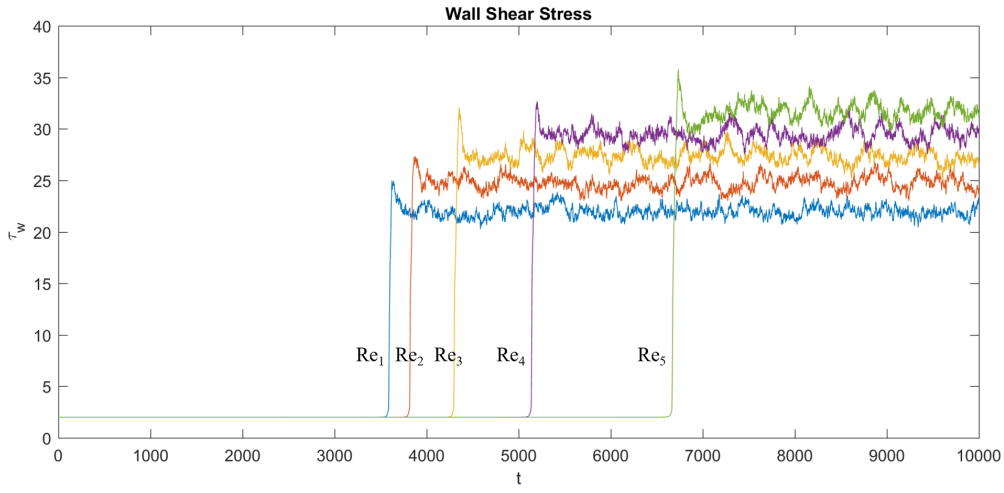

Figure 7: Wall shear stress mean profiles collected at different Reynolds numbers. $Re_1 = 15,000, Re_2 = 17,500, Re_3 = 20,000, Re_4 = 22,500$, and $Re_5 = 25,000$. Note that this figure shows a possible dependency of Reynolds number on the time of transition.

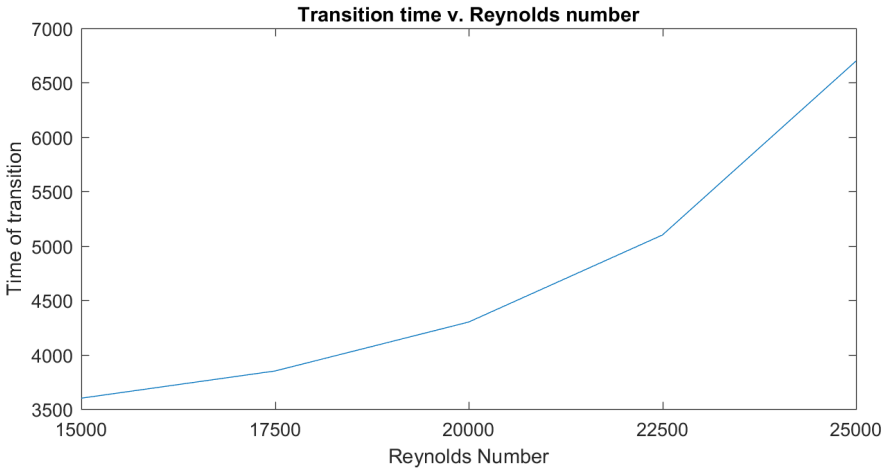

Figure 8: Time of transition vs. Reynolds number. Five data points for the Reynolds number were collected at 2,500 apart. Notice that the form looks almost parabolic, and that the time to transition increases with each increase in Reynolds number.

7 Conclusion

As there is no exact mathematical solution for turbulent flow, "solving" the Navier-Stokes equations computationally is one of the few ways many academics are able to study turbulent and transitional fluids. It is well-documented that the turbulent boundary layer is dominated by what we call coherent structures - vortices, puffs, and waves - and that such structures account for a large portion of turbulent energy production. These structures are an important aspect of the turbulent and transitional boundary layer for several reasons - for instance, many studies aim to reduce turbulent drag using control strategies to manipulate near wall turbulent structures. Additionally, these structures are also a good indicator of when the transition to turbulence begins.

The boundary layer, even in its simplest form, is a topic well-deserving of rigorous study. First introduced by Prandtl, the boundary layer is a very thin layer adjacent to an object moving through fluid in which frictional effects are observed. The Blasius boundary layer is a simple solution to two-dimensional, steady-state, incompressible Navier-Stokes equations. When plotted using numerical schemes, we are able to see how the velocity profiles are structured: as y increases, the velocity increases; and as x increases, the velocity decreases. As the inner velocity eventually goes to zero in turbulent flow, we see the phenomenon called flow separation occur, which causes wake turbulence. In many applications in aerospace, especially, the boundary layer enables us to study properties that may help reduce drag associated with wake turbulence.

A simulation for turbulent wall-bounded flow through a channel was run for the purposes of studying transition to turbulence and coherent structures in transition and turbulent flow. At $Re = 15,000$, wall shear stress remained relatively constant at $\tau_w = 2$, indicating laminar flow, until around time $t = 550$, when transition began to occur. At this point, the wall shear stress jumped dramatically and began

fluctuating, until turbulence is seen to occur after time $t = 600$. Turbulent flow is indicated by the domination of flow structures in the domain - additionally, earlier in the transitional phase, we saw structures (Tollmien-Schlichting waves) which indicated transition.

Several simulations were ran at different Reynolds numbers to observe the effect that increasing the Reynolds number would have on the approximate time of transition. Interestingly, the experiment produced the opposite result of what was expected - a higher Reynolds number resulted in transition actually being delayed. Although this didn't suggest what we assumed it would (that the Reynolds number increasing would lead to the transition occurring faster), it does suggest that there exists a dependency of time of transition on the Reynolds number.

However, the current project's simulation is, overall, consistent with results of previous studies and simulations, as well as with theoretical studies. Further studies and experimentation might address this dependency of Reynolds number on transition time, simulate an object moving through fluid, or study control strategies to manipulate near-wall structures with an end goal of reducing turbulent drag.

References

[1] H. Choi, P. Moin, and J. Kim. Active turbulence control for drag reduction in wall-bounded flows. *Journal of Fluid Mechanics,* 262:75-110, 1994.

[2] Y. Dubief, F. Delcayre. On coherent-vortex identification in turbulence, *Journal of Turbulence*, 1, 2000.

[3] B. Eckhardt, T.M. Schneider, B. Hof, and J. Westerweel. Turbulence Transition in Pipe Flow. *Annual Review of Fluid Mechanics*, 39:447–68, 2007.

[4] S. He, and M. Seddighi. Turbulence in transient channel flow. *J. Fluid Mech.*, 60–102, 2013.

[5] M. Head, and P. Bandyopadhyay. New aspects of turbulent boundary-layer structure. *Journal of Fluid Mechanics*, 107, 297-338, 1981.

[6] J. Jeong, and F. Hussain. On the identification of a vortex. *Journal of Fluid Mechanics*, 285, 69-94, 1995.

[7] J. Jiménez, A. Pinelli. *Journal of Fluid Mechanics*, 389, 335-359, 1999.

[8] S.B. Pope. Turbulent Flows. *Cambridge University Press*, 2000.

[9] S.K. Robinson. Coherent Motions in the Turbulent Boundary Layer. *Annual Review of Fluid Mechanics*, 23:601-39, 1991.

[10] F. Waleffe. *Physics of Fluids*. 9, 883, 1997.

[11] F. Waleffe. *Physics of Fluids*. 15, 1517, 2003.

[12] X. Wu, and P. Moin. Direct numerical simulation of turbulence in a nominally zero-pressure-gradient flat-plate boundary layer. *Journal of Fluid Mechanics*, 630, 5-41, 2009.

[13] J.Z. Wu, A.K. Xiong, and Y.T. Yang. Axial stretching and vortex definition. *Physics of Fluids*, 17: 038108, 2005.

[14] L. Xi, and M. Graham. Turbulent drag reduction and multistage transitions in viscoelastic minimal flow units. *Journal of Fluid Mechanics*, 647, 421-452, 2010.